The 2D extended strike-slip fault segment model with both locking and creeping

Zhenyu Zou[1], Zaisen Jiang[1, 3], Yanqiang Wu[2], Jing Zhao[3], Yueju Cui[1]

[1]Key Laboratory of Earthquake Prediction, Institute of Earthquake Forecasting, CEA, Beijing 100036, China

[2]First Crust Monitoring and Application Center, China Earthquake Administration, Tianjin 300180, China

[3]Institute of Geology, China Earthquake Administration, Beijing 100029, China

Abstract: Based on the classic 2D strike-slip fault model by Savage & Burford (1973), we propose the 2D extended strike-slip fault segment model with both locking and creeping in the interseismic period. First, we give the definition of the fault with locking and creeping (*Lc* fault / *Lc* model); then, the model which meets the definition of the *Lc* fault is constructed and the results of the *Lc* model are numerically simulated which is the same as that of SB73 model except for a scale factor. We further prove the correctness of the results mathematically and give the model of the couple fraction by *Lc* model. The results of *Lc* model illustrate that the not one-to-one correspondence between surface deformation and fault mechanism, which could be more complicated.

Plain language summary: There are two types of fault motion: strike-slip and dip-slip fault. For strike-slip faults, the classic model illustrates that the fault motion is fully locked above certain depth, that is, the fault does not slip at all; the fault motion is fully creeping below the depth, that is, the fault is free creeping without any locking. Although the concept of "both locking and creeping faults" was currently used sometimes, there was no clear definition and physical model for interpreting it. In this paper, we gave the definition and came up with the model for *Lc* faults (both locking and creeping faults). The theoretical curve of the model turned out to be exactly the same as the curve of the classic model (differing by a scale factor only). The results of this study directly indicate that there is no one-to-one correspondence between surface deformation and fault mechanisms. Although this is only theoretical work, it has positive implications for expanding our understanding of fault deformation mechanisms.

1. Introduction

Dislocation theory interpreting the velocity field on the free surface loaded by fault motion has become an important physical model since the elastic rebound theory was put forward (Chinnery, 1963; Matsu'ura et al., 1986; Okada, 1985, 1992; Reid, 1910; Steketee, 2011; Sun & Okubo, 1993, 1998; Wang et al., 2003). The simplest representation of dislocation along an infinitely deep and long strike-slip fault is shown in Figures 1a. The surface velocity of the model represented by a straight and vertical fault in an elastic half-space in which uniform slip equal to the secular relative plate motion occurs on the fault below the depth above which the fault is locked is then given by Savage & Burford (1973) (abbreviated as SB73).

$v = \frac{s}{\pi} \tan^{-1}\left(\frac{x}{d}\right)$ (1)

Where x is the distance from the fault; d is the locking depth, which means that the fault above d is fully locked whereas the one below d is fully creeping; s is the freely creeping below d (Figures 1b). There were two directions in further studies based on the SB73 model. One is that the elastic half-space model is replaced by a layered model that includes at least one viscoelastic layer to represent the asthenosphere, which introduces time-dependent response (Johnson & Fukuda, 2010; Nur & Mavko, 1974; Savage & Prescott, 1978). Savage (1990) further derived the slip distribution on the fault in the equivalent half-space model which produced the same surface deformation as occurred in the lithosphere-asthenosphere model and found that four models, in elastic half-space, fit the geodetic data equally well, which meant that surface velocity distribution did not correspond one-to-one with the fault models; The other is that the couple fraction(Scholz, 2007; McCaffrey, 2002, 2005; McCaffrey et al., 2000; McCaffrey, 2002) , inverted by the negative dislocation, is the extension of locking depth, indicating that the motion of faults above the depth is not fully locking but such a state as locking and creeping coexists. Although the couple fraction has been widely used for inverting the locking state of faults in the interseismic period, no rigorous definition and physical model has been used to describe it at present. In this paper I first define what the fault motion with coexistence of locking and creeping (abbreviated as Lc) is and come up with a 2D extended strike-slip fault model for describing the Lc model based on SB73 model.

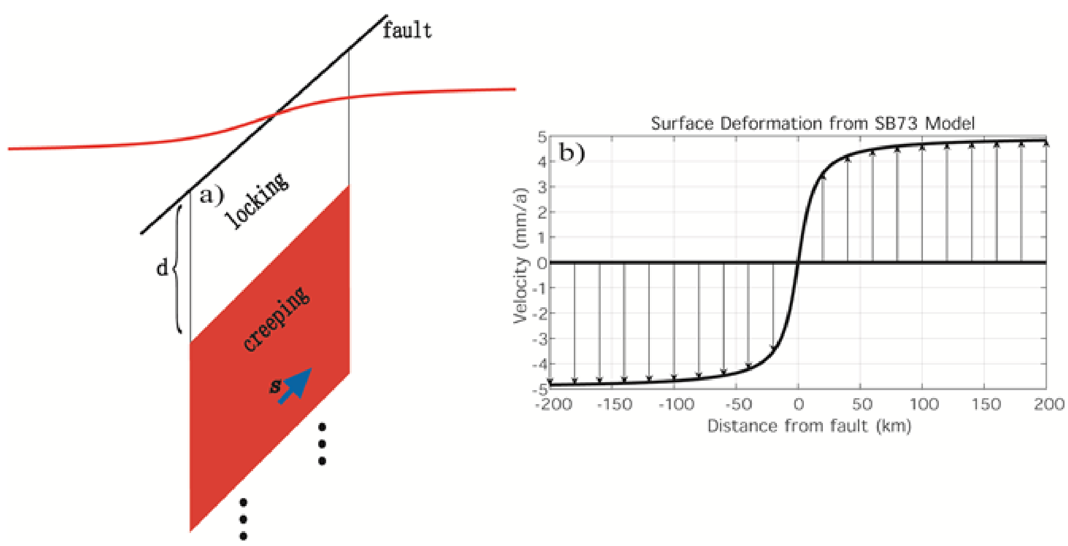

Figure 1.The classic 2D strike-slip fault model (a) and the surface deformation produced (b) (redrawing according to Savage & Burford, 1973). Taking dextral strike-slip fault on which slip rate is 10mm/a and locking depth is 10km as an example.

1. **The definition and model of Lc**

2.1 **Predefinition:** A fault segment which is fully locking is called *Locking segment*; a fault segment which is fully creeping is called *Creeping segment* (Figure 2a)**;** the length of the fault segment is called *Segment length.*

2.2 **Definition of *Lc* model**: the fault segment F_{Lc} is called the *Lc* fault (fault with coexistence of locking and creeping) if there is a fault segment with segment length l on any position of F_{Lc}, no matter how small the value of l is, the segment length of locking and creeping segment in it are both larger than zero as long as l is fixed (Figure 2b). The *Lc* fault means that locking and creeping coexists at any position in the fault segment F_{Lc}.

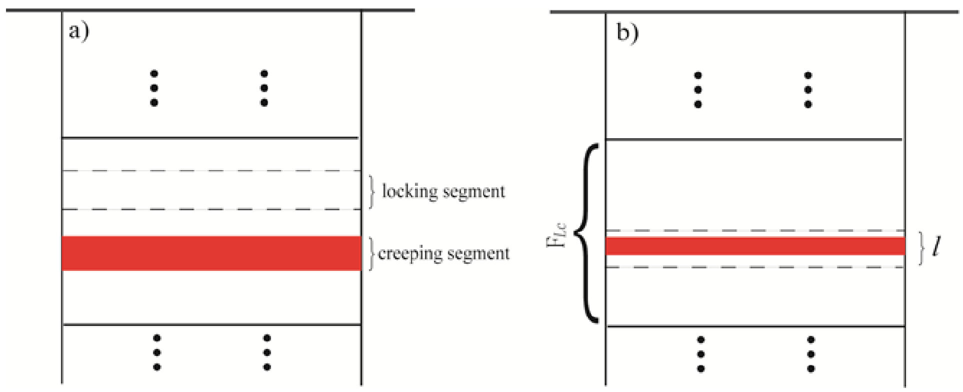

Figure 2.The definition of locking segment and creeping segment (a); the definition of *Lc* fault (b). Red patches represent creeping segment and white patches represent locking segment, dextral strike-slip fault defaulted, hereinafter the same.

2.3 **Construction of *Lc* model:** Firstly, the formula for calculating the slip distribution of the creeping segment of segment length L is introduced as below:

$v = \frac{s}{\pi}\left(\tan^{-1}\frac{x}{d} - \tan^{-1}\frac{x}{d+L}\right)$ (2)

This formula is derived from screw dislocation, which also can be derived by using the SB73 model with the superposition principle (Segall, 2010). Then the formula is used to construct the model that conform the *Lc* definition (Figures 3a):

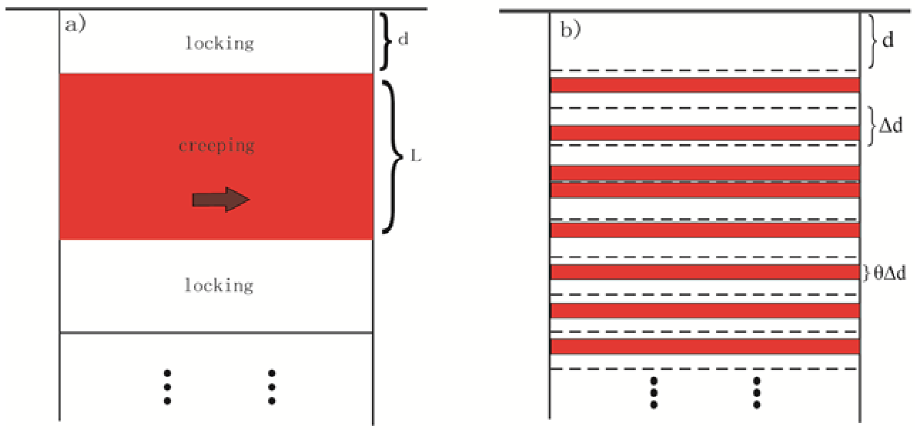

Figure 3.The model of the creeping segment of segment length L (a); the definition of Lc fault (b). Red patches represent creeping segment and white patches represent locking segment, dextral strike-slip fault defaulted, hereinafter the same.

The locking segment is laid from the surface to depth d whereas the fault segment below d is divided into an infinite number of small fault segments, and the segment length of each segment is Δd. Then, the creeping segment is laid on the random position of each of small fault segments (Figures 3b).

$V_{\text{surface}} = \sum_{i=1}^{\infty} \frac{s}{\pi} \left[\tan^{-1}\left(\frac{x}{d_{x_i}}\right) - \tan^{-1}\left(\frac{x}{d_{x_i}+\theta\, d}\right)\right]$ (3)

where $d > 0,\ \ d > 0,\, 0 < \theta < 1$

V_{surface} is the surface deformation generated by the model; d_{x_i} represents the top of the creeping segment in each fault segment, which is a random value in the interval $[d + (i-1)\ d, d + i\ d - \theta\ d]$. Let $\mathrm{Lc}(d, \theta) = \lim_{\,d \to 0} V_{\text{surface}}$.

$\mathrm{Lc}(d, \theta)$ is the formula of model which meets the definition of Lc. We consider a short fault segment with segment length of l in any position of fault segment [d, ∞) , it is always possible that the short fault segment contains both creeping and locking segment when d is small enough as long as l is fixed (No matter how small the l is).

Numerical results show that the simulated curves are sometimes overloaded and sometimes underloaded. When d is small enough, the curves approach a perfect arctangent function, which is exactly θ times the curve of the SB73 model (Figure 4). The Lc model can be proved mathematically that:

$\mathrm{Lc}(d, \theta) = \frac{s}{\pi} \tan^{-1} \frac{x}{d}$ (4)

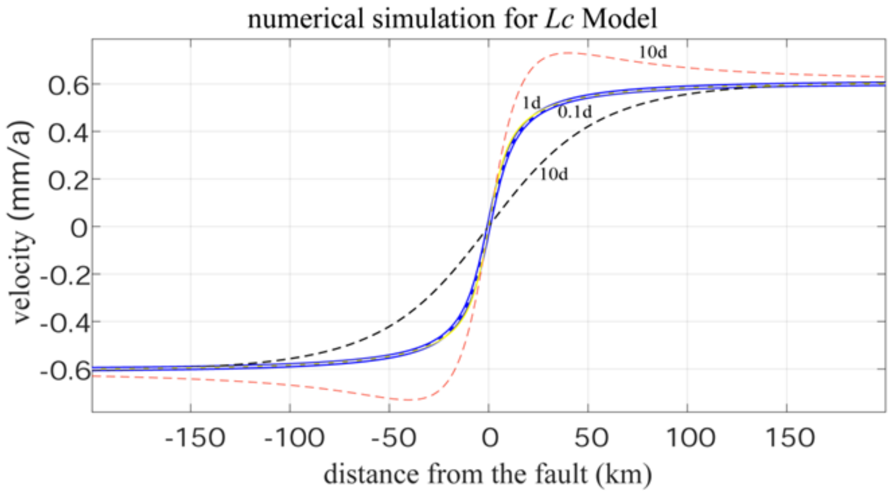

Figure 4.The curves of numerical simulation of Lc model; the default value of θ is 0.4, d is 10km, s is πmm/a; the thick blue line is $\mathrm{Lc}(10, 0.4)$; the red and black dash lines are curves of V_{surface} when d is equal to $10d$, which show that V_{surface} is overloaded or underloaded when approaching to $\mathrm{Lc}(10, 0.4)$ because of the relatively random position of creeping segments in each patches; d of the yellow line which is very close to the $\mathrm{Lc}(10, 0.4)$ is equal to d; the white dash line of which d is equal to $0.1d$ is well fitted with $\mathrm{Lc}(10, 0.4)$.

Formula (4) shows that $\mathrm{Lc}(d, \theta)$ produce the same surface deformation as SB73 model except for a scale factor $\theta (0 \leq \theta \leq 1)$. From the proof process, it can be seen that $\mathrm{Lcf}(d, \theta, L)$ is a more general model than $\mathrm{Lc}(d, \theta)$. Further,

$$\mathrm{Lcf}(0, \theta, L) = \lim_{d \to 0} \mathrm{Lcf}(d, \theta, L) = \frac{\mathrm{s}}{2}\mathrm{sgn}(x) - \frac{\mathrm{s}}{\pi}\tan^{-1}\frac{x}{L} = \frac{\mathrm{s}}{\pi}\tan^{-1}\frac{L}{x}$$

2.4 The model of couple fraction: The definition of couple fraction δ is $\delta = 1 - \frac{s_c}{s}$ (McCaffrey, 2005), which represents the locking degree of fault in the interseimic period. s is said to be secular relative plate motion and s_c represents the slip of non-fully locking of fault. By virtue of negative dislocation (Matsu'ura et al., 1986) which is used for calculating the deformation of secular relative plate motion minus co-seismic motion produced by s, we get surface deformation distribution. The mathematical expression is as follows:

$$v(\delta, d) = \frac{s}{2}\mathrm{sgn}(x) - \frac{\mathrm{s}}{\pi}\tan^{-1}\left(\frac{d}{x}\right)$$

$v(\delta, d)$ represents the deformation of fault on which locking depth is d and couple fraction is δ. $\frac{s}{2}\mathrm{sgn}(x)$ means the secular relative plate motion and $\frac{\mathrm{s}}{\pi}\tan^{-1}\left(\frac{d}{x}\right)$ means the co-seismic motion produced by s.

$$\therefore\ v(\delta, d) = \frac{s}{2}\mathrm{sgn}(x) - \left[\frac{s}{2}\tan^{-1}\left(\frac{d}{x}\right) - \frac{(1-\delta)s}{\pi}\tan^{-1}\left(\frac{d}{x}\right)\right]$$

$= \mathrm{Lcf}(0, 1-\delta, d) + \frac{s}{\pi}\tan^{-1}\left(\frac{x}{d}\right)$ (5)

The result shows that the deformation produced by fault of couple fraction is the total deformation of SB73 and Lcf$(0, \theta, d)$ (Figure 5). There $\theta = 1-\delta$. Thus, we have the model of the couple fraction.

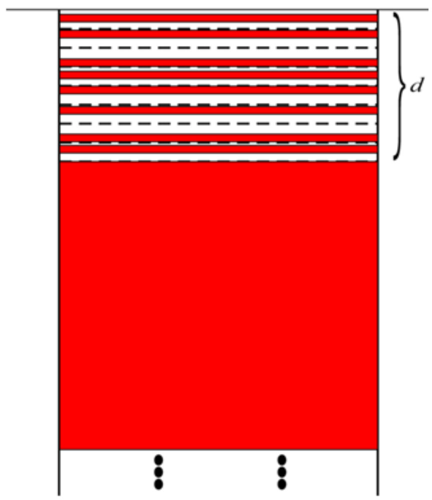

Figure 5.The model of the couple fraction is equal to sum of SB73 and Lcf$(0, \theta, d)$

1. **Disscusion:**

Fault motion with both locking and creeping could be of practical significance that the fault with couple fraction is a proper example. The couple fraction is a special case of the *Lc* model, which is the locking segment of the SB73 model changed into the *Lc* mode. The *Lc* model is more general than the couple fraction. For instance, Lc(d, θ) means that creeping segment of the SB73 model changed into *Lc* mode. More complex models could be constructed by superposition principle and Lcf(d, θ, L) with different d and θ. Since the surface deformation generated by *Lc* model is theoretically identical to the one by SB73 (only differs a scale factor), it is difficult to determine whether the deformation mechanism of the fault is caused by the *Lc* or the SB73 from the surface GNSS velocity field profile only (even if this profile has good arctangent function characteristics). However, it can be seen from the numerical simulation results approaching the theoretical curve, when d is not very small, that is, the locking and creeping segment have obvious segmentation features, the surface deformation could be overloaded in the near field of the fault sometimes in the interseismic period. Although there are many factors affecting the deformation of near field of fault, it is not uncommon that the velocities of individual stations on the near field of the fault are overloaded in some profile results (Smith et al., 2011; Vernant, 2015)(In the interseismic period, curves may also be underloaded, but they are easily fitted by SB73.)

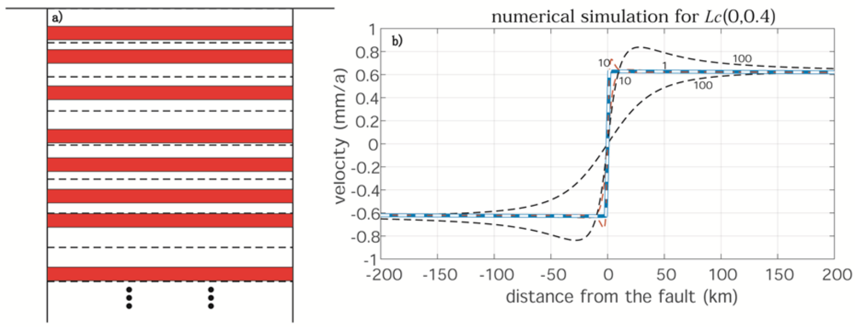

Figure 6.The model of $\mathrm{Lc}(0,\theta)$(a); the numerical simulation for $\mathrm{Lc}(0,0.4)$(b), the default value of θ is 0.4, d is 0.01km, s is πmm/a; the thick blue line is $\mathrm{Lc}(0,0.4)$; the black dash lines are curves when d is equal to 100km, which show that surface deformation is overloaded or underloaded when approaching to $\mathrm{Lc}(0,0.4)$; d of the red lines which is close to the $\mathrm{Lc}(0,0.4)$ is equal to 10km, which are also overloaded and underloaded in the near field of fault; the white dash line of which d is equal to 1km is completely fitted with $\mathrm{Lc}(0,0.4)$.

Savage (1990) derived the surface deformation on the fault in the half-space model which produced the same deformation as occurred in the lithosphere-asthenosphere model and found that four equivalent models yielded satisfactory approximations to the velocity field on San Andreas. He stated that: "Even high-quality geodetic measurements across a transform fault are incapable of defining the deformation mechanism at depth." The results in this paper could be additional corroboration for his statement: the deformation of *Lc* and SB73 model are theoretically the same, so surface deformation and fault mechanisms are probably not one-to-one correspondence. Such assumption in previous studies as fault is fully creeping below certain depth if count is not taken of shallow creep near the surface should be further studied, because the *Lc* model which can produce the same deformation does not satisfy the assumption sometimes. Here we give an extreme and counter-intuitive example based on *Lc* model to illustrate the not one-to-one correspondence between surface deformation and fault mechanisms: Let $d \to 0$, $\therefore \mathrm{Lc}(d,\theta) \to \frac{s}{2}\mathrm{sgn}(x)$ (Figures 6a). The result shows that fault turns out be creeping at slip rate s while the length of sum of locking segments tends to infinity and locking segments seem to be anywhere on the fault, which illustrates that even the motion that appears to be fully creep cannot directly indicate that the fault is only creeping without locking(Figures 6b). This result is a theoretical result, and currently only illustrates that a fault that seems to be completely creeping could be a special way of *Lc* fault motion, but how does the *Lc* fault accumulate deformation in the locking segment in the interseismic period and how does the co-seismic deformation distribute?

Further research is needed.

1. **Conclusion:**

This study proposed the extended 2D strike-slip fault model with both locking and creeping. We firstly gave the definition of *Lc* fault, and constructed the model which met the definition. The result of *Lc* model showed the same deformation as that of SB73 model except for a scale factor. Then we gave the model of couple fraction based on *Lc* model. So far *Lc* model is just a theoretical model, two major issues need to be further studied if practical application could be taken into account: one is that slip rate fitted with GNSS velocity field could be lower than the real slip rate of the fault due to $\theta(0 \leq \theta \leq 1)$ of *Lc* fault mechanism in the interseismic period. However, what the true and accurate slip rate of the fault is could be difficult to get; the other is that the strain accumulation of the *Lc* fault, the evolution of the locking segment, and the distribution of the coseismic deformation need to be further studied. Anyway, the *Lc* model expands understanding of relationship between surface deformation and fault mechanisms.

Acknowledgement

The core ideas of the proof about *Lc* model were provided by three moderators (Czhang271828, kuing and TSC999) on the online mathematics forum (http://kuing.orzweb.net/viewthread.php?tid=8497&extra=page%3D1%26amp%3Bfilter%3Dtype%26amp%3I This research was supported by the National Natural Science Foundation of China (41904092 and 41974011), the National Key Research and Development Program of China (2018YFE0109700 and 2019YFC1509203) and the Basic Research Project of the Institute of Earthquake Forecasting, China Earthquake Administration (2020IEF0506). Matlab software was used to prepare some of the figures.

Data Availability Statement

No actual data is used in this study; the images of GNSS velocity profiles mentioned in the discussion section are available on Smith (doi.org/10.1029/2010JB008117) and Vernant (doi.org/10.1016/j.tecto.2015.01.013), respectively.

References:

C. H. Scholz. (2007). The Mechanics of Earthquakes and Faulting: (C. H. Scholz). *Environmental & Engineering Geoscience - ENVIRON ENG GEOSCI*, *13*, 81–83. https://doi.org/10.2113/gseegeosci.13.1.81Chinnery, M. (1963). The stress changes that accompany strike-slip faulting. *Bull. Seismol. Soc. Am.*, *53*.Johnson, K. M., & Fukuda, J. (2010). New methods for estimating the spatial distribution of locked asperities and stress-driven interseismic creep on faults with application to the San Francisco Bay Area, California. *Journal of Geophysical Research: Solid Earth*, *115*(B12). https://doi.org/10.1029/2010JB007703Matsu'ura, M., Jackson, D. D., & Cheng, A. (1986). Dislocation model for aseismic crustal deformation at

Hollister, California. *Journal of Geophysical Research: Solid Earth*, *91*(B12), 12661–12674. https://doi.org/10.1029/JB091iB12p12661McCaffrey, R. (2005). Block kinematics of the Pacific-North America plate boundary in the southwestern US from inversion of GPS, seismological, and geologic data. *Journal of Geophysical Research*, *110*. https://doi.org/10.1029/2004JB003307McCaffrey, R., Long, M. D., Goldfinger, C., Zwick, P. C., Nabelek, J. L., Johnson, C. K., & Smith, C. (2000). Rotation and plate locking at the Southern Cascadia Subduction Zone. *Geophysical Research Letters*, *27*(19), 3117–3120. https://doi.org/10.1029/2000GL011768Nur Amos & Mavko Gerald. (1974). Postseismic Viscoelastic Rebound. *Science*, *183*(4121), 204–206. https://doi.org/10.1126/science.183.4121.204Okada, Y. (1985). Surface deformation due to shear and tensile faults in a half-space. *Bulletin of the Seismological Society of America*, *75*(4), 1135–1154. https://doi.org/10.1785/BSSA0750041135Okada, Y. (1992). Internal deformation due to shear and tensile faults in a half-space[J]. *Bull Seism Soc Amer*, *82*, 1 018-1 040. https://doi.org/10.1785/BSSA0820021018Reid, H. F. (1910). The machanism of the earthquake, in The California Earthquake of April 18, 1906. *Report of the State Earthquake Investigation Commission*, *2*.Robert McCaffrey. (2002). Crustal Block Rotations and Plate Coupling. *Plate Boundary Zones*. Retrieved from https://agupubs.onlinelibrary.wiley.com/doi/abs/10.1029/GD030p0101Savage, J., & Burford, R. (1973). Geodetic Determination of Relative Plate Motion in Central California. *Journal of Geophysical Research*, *78*, 832–845. https://doi.org/10.1029/JB078i005p00832Savage, J. C. (1990). Equivalent strike-slip earthquake cycles in half-space and lithosphere-asthenosphere earth models. *Journal of Geophysical Research: Solid Earth*, *95*(B4), 4873–4879. https://doi.org/10.1029/JB095iB04p04873Savage, J. C., & Prescott, W. H. (1978). Asthenosphere readjustment and the earthquake cycle. *Journal of Geophysical Research: Solid Earth*, *83*(B7), 3369–3376. https://doi.org/10.1029/JB083iB07p03369Segall, P. (2010). *Earthquake and Volcano Deformation*. Princeton University Press,.Smith-Konter, B. R., Sandwell, D. T., & Shearer, P. (2011). Locking depths estimated from geodesy and seismology along the San Andreas Fault System: Implications for seismic moment release. *Journal of Geophysical Research: Solid Earth*, *116*(B6). https://doi.org/10.1029/2010JB008117Steketee, J. (2011). On Volterra' 's Dislocations in a Semi-Infinite Elastic Medium. *Canadian Journal of Physics*, *36*, 192–205. https://doi.org/10.1139/p58-024Sun, W., & Okubo, S. (1993). Surface potential and gravity changes due to internal dislocations in a spherical earth—I. Theory for a point dislocation. *Geophysical Journal International*, *114*(3), 569–592. https://doi.org/10.1111/j.1365-246X.1993.tb06988.xSun, W., & Okubo, S. (1998). Surface potential and gravity changes due to internal dislocations in a spherical earth—II. Application to a finite fault. *Geophysical Journal International*, *132*(1), 79–88. https://doi.org/10.1046/j.1365-246x.1998.00400.xVernant, P. (2015). What can we learn from 20years of interseismic GPS measurements across strike-slip faults? *Tectonophysics*, *644–645*, 22–39. https://doi.org/10.1016/j.tecto.2015.01.013Wang, R., Martín, F., & Roth, F. (2003). Computation of deformation induced by earthquakes in a multi-layered elastic crust - FORTRAN programs EDGRN/EDCMP (vol 29, pg 195, 2003). *Computers & Geosciences*, *29*, 195–207. https://doi.org/10.1016/S0098-3004(02)00111-5